

Tunable Magnon-Photon Coupling by Magnon Band Gap in a Layered Hybrid Perovskite Antiferromagnet

Yi Li,^{1,*} Timothy Draher,^{1,2} Andrew H. Comstock,³ Yuzan Xiong,^{4,1} Md Azimul Haque,⁵ Elham Easy,⁶ Jiang-Chao Qian,⁷ Tomas Polakovic,⁸ John E. Pearson,¹ Ralu Divan,⁹ Jian-Min Zuo,⁷ Xian Zhang,⁶ Ulrich Welp,¹ Wai-Kwong Kwok,¹ Axel Hoffmann,⁷ Joseph M. Luther,⁵ Matthew C. Beard,⁵ Dali Sun,^{3,†} Wei Zhang,^{4,‡} and Valentine Novosad^{1,§}

¹*Materials Science Division, Argonne National Laboratory, Argonne, IL 60439, USA*

²*Northern Illinois University, Department of Physics, DeKalb Illinois, 60115, USA*

³*Department of Physics and Organic and Carbon Electronics Laboratory (ORACEL), North Carolina State University, Raleigh, NC 27695 USA*

⁴*Department of Physics and Astronomy, University of North Carolina, Chapel Hill, NC 27599, USA*

⁵*Chemistry and Nanoscience Center, National Renewable Energy Laboratory, Golden, CO 80401, USA*

⁶*Department of Mechanical Engineering, Stevens Institute of Technology, Hoboken, NJ 07030, USA*

⁷*Department of Materials Science and Engineering, University of Illinois Urbana-Champaign, Urbana, IL 61820, USA*

⁸*Physics Division, Argonne National Laboratory, Lemont, IL 60439, USA*

⁹*Center for Nanoscale Materials, Argonne National Laboratory, Argonne, IL 60439, USA*

(Dated: July 28, 2023)

Tunability of coherent coupling between fundamental excitations is an important prerequisite for expanding their functionality in hybrid quantum systems. In hybrid magnonics, the dipolar interaction between magnon and photon usually persists and cannot be switched off. Here, we demonstrate this capability by coupling a superconducting resonator to a layered hybrid perovskite antiferromagnet, which exhibits a magnon band gap due to its intrinsic Dzyaloshinskii-Moriya interaction. The pronounced temperature sensitivity of the magnon band gap location allows us to set the photon mode within the gap and to disable magnon-photon hybridization. When the resonator mode falls into the magnon band gap, the resonator damping rate increases due to the nonzero coupling to the detuned magnon mode. This phenomena can be used to quantify the magnon band gap using an analytical model. Our work brings new opportunities in controlling coherent information processing with quantum properties in complex magnetic materials.

Hybrid quantum systems [1–3] offer an important pathway for harnessing different natural advantages of complementary quantum systems, leveraging the distinct properties of their constituent excitations. The fundamental excitations of magnetically ordered materials, i.e. magnons, provide efficient coupling with other excitations [4, 5], such as microwave photons [6–12], acoustic phonons [13–16], and magnons themselves [17–24], therefore holding promise for future integration with diverse quantum modules [25–28]. In addition, coherent magnon interactions exhibit great controllability in different aspects, such as polarization [11], mode profile [21], phase [29–32] and layer structure [20], allowing for implementation of coherent magnon operations [33]. Recent demonstrations of coherent magnon-magnon coupling with controllable coupling strength by frequency detuning [34, 35] have further expanded the capability of distributed hybrid magnonic networks [4].

Despite its controllability, which is largely based on extrinsic control of magnetic systems, the intrinsic magnetic properties are rarely explored for manipulating coherent magnon interactions. To date, landmark demonstrations of hybrid magnonics have been centered on the ferrimagnetic insulator yttrium iron garnet (YIG) [6, 8–10, 36] or metallic magnets such as NiFe [11, 12]. Their relatively simple and rigid chemical and magnetic struc-

tures limit the potential for developing highly tunable hybrid systems. On the other hand, the recent two-dimensional (2D) organic layered magnets [37] offer distinct advantages in their structure-enabled topological chirality and symmetry breaking [38]. One nice class of materials is 2D magnetic hybrid organic-inorganic perovskites (HOIPs) possessing both superior structural versatility and long-range magnetic order [39–42]. They usually exhibit an interlayer antiferromagnetic (AFM) coupling [43], inducing the acoustic and optical magnon modes [19, 44] in the gigahertz (GHz) frequency range. In addition, the structural symmetry breaking leads to Dzyaloshinskii-Moriya interaction (DMI) [45], causing a finite spin canting [46, 47] and creating an intrinsic magnon band gap where the acoustic and optical modes intersect [48]. This is fundamentally different from the magnon band gap induced by an external field [49][19, 21–24, 50] in that the DMI has provided an intrinsic effective field for magnon-magnon coupling without the need of external field. Furthermore, the large sensitivity of the magnon band gap to small temperature change can lead to new opportunities of modulating coherent magnonic coupling.

[51] In this Letter, we report a hybrid magnonic system consisting of a 2D HOIPs, $(\text{CH}_3\text{CH}_2\text{NH}_3)_2\text{CuCl}_4$ (CuEA) [48], coupled to a superconducting resonator. The

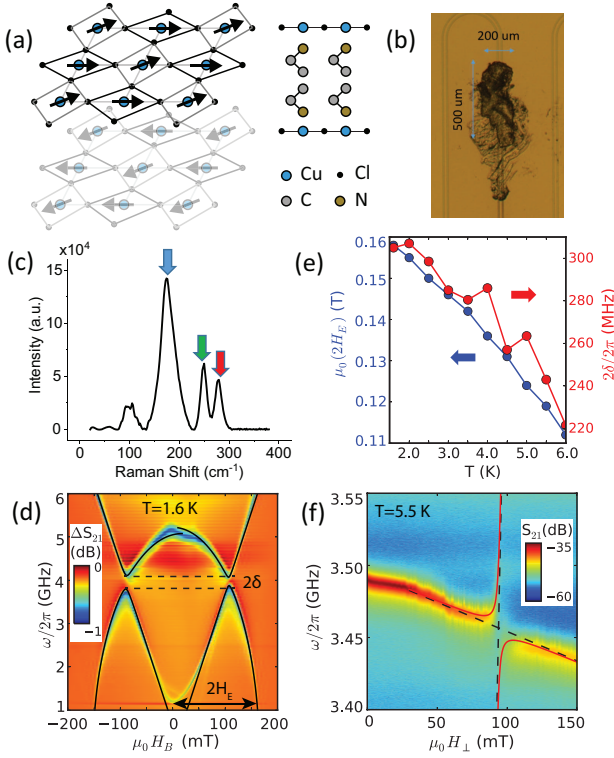


FIG. 1. (a) Lattice structure of layered perovskite antiferromagnet Cu-EA, with Cu filling the octahedral sites of Cl and the antiferromagnetic layers separated by the $\text{CH}_3\text{CH}_2\text{NH}_3$ molecules. (b) Optical microscope image of a small Cu-EA flake mounted onto a CPW superconducting resonator. (c) Raman spectroscopy of Cu-EA showing the high-frequency octahedral modes and the low-frequency organic structure modes. (d) Broad-band ferromagnetic resonance spectra of a large Cu-EA crystal measured at 1.6 K, which is used to extract the magnon band gap 2δ , the interlayer exchange field $2H_E$, and magnon damping rate κ_m . The colorbar shows the signals ΔS_{21} after background subtraction. (e) Extracted $2H_E$ (magenta) and 2δ (red) as a function of T . (f) Mode anticrossing between magnons and photons at 5.5 K, with $H_B \perp h_{\text{rf}}^y$. The colorbar shows the signals S_{21} in absolute values. The red curves are the fits with $g/2\pi = 45$ MHz. The black dashed lines denote the magnon and photon modes without interaction.

high sensitivity of the superconducting resonator enables coherent magnon-photon coupling and avoided crossing with a small Cu-EA flake. By changing the temperature of the sample, the location of the DMI-induced magnon band gap can be adjusted so that the resonator photon mode completely falls into the gap and cancels the mode hybridization. At the non-hybridized state, the magnetic interaction with the resonator causes the resonator linewidth to broaden. Using our developed analytical model, the narrow-band linewidth broadening measurements can be used to extract the magnon band gap, which quantitatively agrees with the broad-band FMR measurements. Our results highlight the opportunity of manipulating coherent mode hybridization

with new quantum materials and probing their complex magnonic dispersion with narrow-band microwave characterizations.

The chemical structure of Cu-EA features corner-sharing halogen (Cl) octahedra with the Cu atom situated at the center, as shown in Fig. 1(a). The canted inorganic CuCl_4^{2-} octahedral structures allow for intralayer long-range magnetic order with superexchange Cu-Cl-Cu interactions, while the interlayer organic cations modulate the interlayer antiferromagnetic (AFM) coupling [43]. Raman spectroscopy of the Cu-EA [52] confirms the vibration modes of the octahedral structure (at 175, 250, and 280 cm^{-1}) and the organic cation (at 100 cm^{-1}) [53], as shown in Fig. 1(c). We have also conducted Inductively Coupled Plasma (IPC) spectroscopy on the sample, showing accurate stoichiometry of the elemental weight as compared with the chemical structure [54].

Fig. 1(d) shows the broad-band ferromagnetic resonance of a large Cu-EA crystal at 1.6 K at parallel pumping condition, i.e. $\mu_0 H_B \parallel h_{\text{rf}}^y$ as illustrated in Fig. 2(b). Both the acoustic and optical modes are measured, which can be formulated as [19]:

$$\omega_a = \mu_0 \gamma \sqrt{2H_E(2H_E + M_{\text{eff}})} \frac{H}{2H_E} \quad (1)$$

$$\omega_o = \mu_0 \gamma \sqrt{2H_E M_{\text{eff}} \left(1 - \frac{H^2}{4H_E^2}\right)} \quad (2)$$

where H_E is the interlayer exchange coupling field, M_{eff} is the effective magnetization which contributes to the perpendicular demagnetization field, and $\gamma/2\pi = (g_e/2) \times 28$ GHz/T is the gyromagnetic ratio, with g_e as the g -factor of the magnetization. Clear avoided crossing gaps between the two modes show the existence of magnon band gap around 4 GHz. The coupled magnon spectra can be fitted to the hybrid mode expression $\omega_{\pm}^{mm} = (\omega_a + \omega_o)/2 \pm \sqrt{(\omega_a - \omega_o)^2/4 + \delta^2}$, where δ is the magnon-magnon coupling strength. The fitting curves are plotted in Fig. 1(d). The extracted parameters are $\mu_0 H_E = 0.16$ T, $\mu_0 M_{\text{eff}} = 80$ mT, $g_e = 2.3$, and $\delta/2\pi = 150$ MHz. Note that the actual saturation magnetization of Cu-EA can be larger than M_{eff} because the shape of the sample crystal is not a perfect two-dimension system and the perpendicular demagnetization factor can be smaller than one. The strong magnon-magnon coupling observed in Cu-EA at parallel pumping condition, which is absent in other layered [19] or synthetic [21, 22] antiferromagnets at the same pumping condition, is caused by the spontaneous canting of the octahedral CuCl_4^{2-} spin sites from their chiral DMI and the resultant overlap between the acoustic and optical modes [48]. Fig. 1(e) shows the temperature dependence of extracted $2H_E$ and the magnon band gap 2δ from Fig. 1(d). With the same y -axis proportion ratio in Fig. 1(e), a good overlap of H_E and δ shows that they

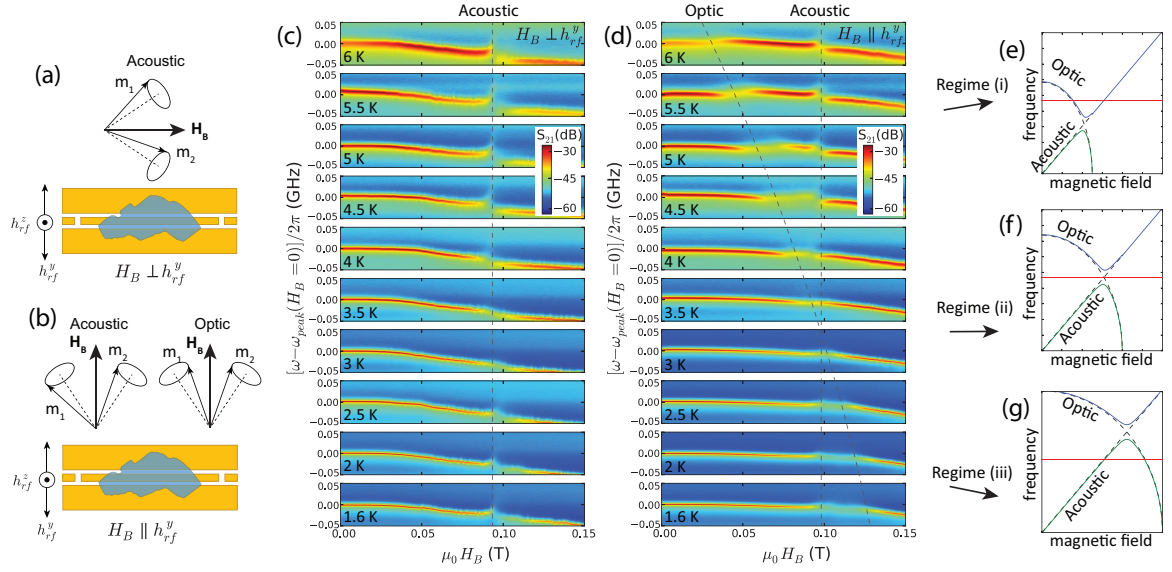


FIG. 2. (a-b) Illustration of two different in-plane field alignments and their selective mode excitations. In (a), $\mu_0 H_B \perp h_{rf}^y$ and only the acoustic mode is excited. In (b), $\mu_0 H_B \parallel h_{rf}^y$ and both the acoustic and optical modes are excited. (c-d) Temperature dependence of the magnon-phonon coupling evolutions from 1.5 to 6 K with two different magnetic field alignments. All the dispersion centered at the resonator photon mode ($\omega_p/2\pi \approx 3.5$ GHz). Dashed curves are guide to eye for the acoustic mode crossing the resonator mode at $\mu_0 H_a = 95$ mT and the optical mode crossing the resonator mode at different fields. (e-g). Illustration of the three regimes where the resonator mode is (e) above, (f) within, and (g) below the magnon band gap.

are proportional to each other at different temperatures. This suggests that the DMI-induced spin canting shares a similar mechanism with the interlayer exchange coupling in Cu-EA. The magnon damping rate, κ_m , of the acoustic and optical modes are also extracted and are found to be weakly frequency and temperature dependent. In the range of 2-5 GHz, $\kappa_m/2\pi \sim 50$ MHz for the acoustic mode and ~ 80 MHz for the optical mode; see the Supplemental Materials for details [54].

To feature the sensitivity of the superconducting resonator to small magnetic crystals, we precisely transfer a thin Cu-EA flake with lateral dimensions of $500 \mu\text{m} \times 200 \mu\text{m}$ and a thickness of $40 \mu\text{m}$ onto the center of a half-wavelength NbN coplanar waveguide (CPW) superconducting resonator with a signal line width of $20 \mu\text{m}$, as shown in Fig. 1(b). The dimension matching between the signal line and the flake thickness allows for optimal coupling of the magnon excitations to the resonator. The loaded superconducting resonator exhibits a sharp peak at $\omega_p/2\pi = 3.5$ GHz and a zero-field half-width half-maximum linewidth of $\kappa_p/2\pi = 0.4$ MHz at 1.6 K, which corresponds to a quality factor of $\omega_p/2\kappa_p = 4400$.

The maximum mode splitting happens at 5.5 K between the acoustic magnon mode of Cu-EA and the resonator photon mode, shown in Fig. 1(f). The peak positions of the avoided crossing can be fitted to the hybrid modes [6]:

$$\omega_{\pm}^{mp} = (\omega_m + \omega_p)/2 \pm \sqrt{(\omega_m - \omega_p)^2/4 + g^2} \quad (3)$$

where ω_m is the magnon frequency, ω_p is the photon fre-

quency, and g is the magnon-photon coupling strength due to dipolar interaction. The field dependence of ω_p can be extracted from the linear extrapolation of the background, and the field dependence of ω_m can be obtained from the broad-band FMR spectrum. Fits to Eq. (3) yield $g/2\pi = 45$ MHz. Using the damping rates of $\kappa_p/2\pi = 2.7$ MHz for the superconducting resonator at 5.5 K and $\kappa_m/2\pi = 50$ MHz for the Cu-EA acoustic mode, we obtain a cooperativity of $C = g^2/\kappa_p\kappa_m = 15$. We note that even though the cooperativity becomes higher at lower temperature, e.g. 1.6 K, because of the much lower κ_p , the real bottleneck of strong magnon-photon coupling is the ratio g/κ_m , which is maximized as 0.95 at 5.5 K. The strong coupling regime requires both g/κ_m and g/κ_p to be greater than one [9]. See the Supplemental Materials for the temperature dependence of κ_p and κ_m [54].

Next, we investigate the temperature dependence of the magnon-photon interactions. Shown in Figs. 2(a) and (b), the signal line of the resonator generates both the in-plane and perpendicular Oersted fields, h_{rf}^y and h_{rf}^z , respectively. In the orthogonal pumping condition ($\mu_0 H_B \perp h_{rf}^y$), the Oersted field components h_{rf}^y and h_{rf}^z only couple to the acoustic mode. In the parallel pumping condition ($\mu_0 H_B \parallel h_{rf}^y$), h_{rf}^y couples to the acoustic mode and h_{rf}^z couples to the optical mode. Thus, the field alignment allows for selective excitation of the acoustic mode in Fig. 2(c), or the mutual excitation of both modes in Fig. 2(d). The interaction with the acoustic mode is manifested by an avoided crossing at a con-

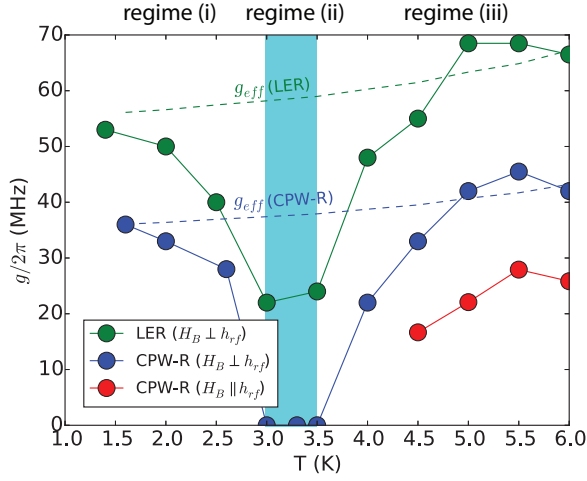


FIG. 3. Extracted effective magnon-photon coupling g as a function of T . The resonator mode is within the magnon band gap between 3 and 3.5 K, yielding $g = 0$.

stant field of $\mu_0 H_a = 95$ mT for both pumping geometries. The optical mode found in Fig. 2(d) shows a large temperature-dependent drift of its location, as marked by the dashed curves. The reversed anticrossing compared with the acoustic mode shows that the magnon frequency decreases as the field rises, agreeing with the feature of the optical mode as shown in Fig. 1(d).

Due to the tunability of H_E , the center frequency of the magnon band gap changes rapidly with temperature in the range from 1.5 to 6.0 K, therefore, allowing the resonator mode (much less sensitive to temperature) to intercept with the magnon band gap while maintaining a nearly constant quality factor. Three regimes of the magnon-photon coupling between the Cu-EA flake and the superconducting resonator are observed, with the relation between the magnon band gap and the resonator mode shown in Figs. 2(e-g). In regime (i) ($T > 3.5$ K), the magnon band gap is below the superconducting resonator frequency [Fig. 2(e)]. The resonator photon mode coherently interacts with the acoustic mode in Fig. 2(c), and both the acoustic and optical modes in Fig. 2(d). In regime (ii) ($3.5 \geq T \geq 3$ K), the acoustic and optical magnon modes cross each other and form the magnon band gap at the superconducting resonator mode frequency. This causes the resonator mode to fall inside the magnon band gap, leading to a moderate change of the peak amplitude and linewidth without peak frequency shift around 95 mT. In regime (iii) ($T < 3$ K) where the magnon band gap is above the resonator mode, the acoustic mode resumes its anticrossing-like interaction with the resonator mode. In addition, for the $\mu_0 H_B \parallel h_{rf}^y$ geometry where the optical mode also interacts with the resonator mode [Fig. 2(d)], the regime between the optical and acoustic modes are blurred, as shown in regimes (i) and (iii). This indicates that one of the two acoustic-

optical hybrid magnonic modes is still near the resonator mode and maintains the magnon-photon interaction.

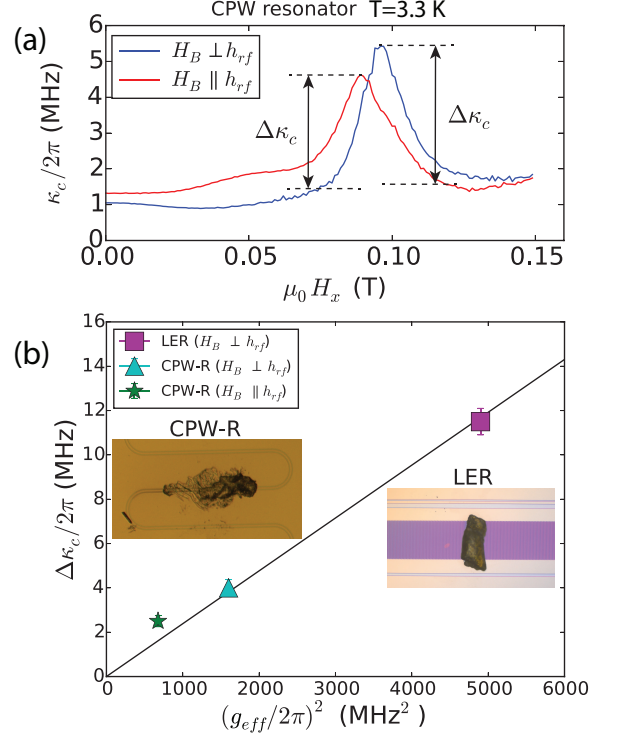


FIG. 4. (a) Superconducting resonator linewidth κ_c as a function of H_B at $T = 3.3$ K, where the resonator mode is inside the magnon band gap. (b) SC resonator linewidth change $\Delta\kappa_c$ as a function of g_{eff}^2 for the CPW and LER resonator designs. Error bars denote the uncertainty of base resonator linewidth drift under external magnetic fields. The red line is a fit to Eq. 4, with the slope quantifying the magnon band gap 2δ .

Figure 3 summarizes extracted magnon-photon coupling strength, g , as a function of T . To verify the phenomena, we have also coupled another Cu-EA crystal to a lumped-element resonator (LER) [55]. This allows for a larger magnon-photon coupling strength while maintaining the same magnon band gap. For both the CPW resonator and LER, g quickly decreases in regime (ii) due to mode degeneracy breaking between the magnon mode and the resonator photon mode. The zero coupling strength for the CPW resonator is manifested by the continuous evolution of resonator peak without mode anticrossing, as shown in Fig. 2(c-d). For the LER, a finite g can still be extracted in regime (ii) which is due to non-perfect centering of the resonator mode in the magnon band gap when then magnon-photon coupling is large. The maximal acoustic mode coupling strengths for the CPW resonator are $g_{\text{CPW}}^{\perp}/2\pi = 45$ MHz for $\mu_0 H_B \perp h_{rf}^y$ and $g_{\text{CPW}}^{\parallel}/2\pi = 28$ MHz for $\mu_0 H_B \parallel h_{rf}^y$ at 5.5 K. Their difference quantifies the coupling ratio of the acoustic magnon mode between the in-plane (h_{rf}^y) and perpendicular (h_{rf}^z) Oersted fields from

the CPW: at $\mu_0 H_B \perp h_{\text{rf}}$, both h_{rf}^y and h_{rf}^z couple to the acoustic mode, while at $\mu_0 H_B \parallel h_{\text{rf}}$, only h_{rf}^z couples to the acoustic mode. The ratio can be calculated as $h_{\text{rf}}^y/h_{\text{rf}}^z = \sqrt{(g_{\text{CPW}}^\perp)^2 - (g_{\text{CPW}}^\parallel)^2}/g_{\text{CPW}}^\perp = 1.25$. For the LER, the obtained ratio is 1.23. This suggests that h_{rf}^z plays an important role in magnon-photon coupling. When the magnon band gap is far from the resonator mode (e.g. 1.5 K and 6 K), a reduction of g from 6 K to 1.5 K reflects the change of coupling efficiency between the Oersted field and the canted magnetization at different biasing field directions. We plot the calculated prediction of the effective magnon-photon coupling, g_{eff} , for the acoustic magnon mode without considering the magnon band gap [54], and the trend nicely captures the experiment at low and high temperatures.

We show that the magnon band gap of Cu-EA can be quantitatively extracted from the modulated magnon-photon interaction. When the resonator mode is inside the magnon band gap in regime (ii), the interaction between the magnon and photon modes leads to a linewidth broadening of the resonator photon mode. Such an effect has been previously observed in magnon-magnon coupled bilayers in the Purcell regime [56–59]. We develop an analytical model for quantifying the change of photon linewidth by considering two detuned magnon mode coupled to the photon mode. The photon damping rate κ_c can be expressed as:

$$\kappa_c = \kappa_{c0} + (g_{\text{eff}})^2 \frac{\kappa_m}{\kappa_m^2 + \delta^2}, \quad (4)$$

where κ_{c0} is the intrinsic photon damping rate, g_{eff} is the effective magnon-photon coupling strength as plotted in Fig. 3, κ_m is the magnon damping rate, and 2δ is the magnon-magnon band gap. The detailed derivation of the model is included in the Supplemental Materials [54]. Note that the information of g_{eff} needs to be obtained from regime (iii) where mode anticrossing between the magnon and photon modes are resumed. Eq. (4) shows that the change of linewidth $\Delta\kappa_c = \kappa_c - \kappa_{c0}$ is proportional to $(g_{\text{eff}})^2$, with the slope determined by two intrinsic magnon characteristics of the Cu-EA: κ_m and 2δ . With two completely different superconducting resonator designs, i.e., the CPW resonator and LER, we find that the extracted $\Delta\kappa_c$ nicely follows the linear dependence of $(g_{\text{eff}})^2$, with a slope of $(210 \text{ MHz})^{-1}$. For κ , we take the average of the acoustic and optical modes, as $\kappa_m/2\pi = 65 \text{ MHz}$. The magnon band gap is calculated to be $\delta/2\pi = 152 \text{ MHz}$, which is close to the value in Fig. 1(e) as 140 MHz around 3.5 K. Thus, we confirm the validity of this new technique for quantifying the magnon band gap δ of a small magnetic flake with a highly sensitive superconducting microwave resonator, where the linewidth change of the resonator mode acts as a probe to interact with the acoustic-optical hybrid magnon modes.

In summary, we demonstrate tunable magnon-photon

coupling by adjusting the intrinsic magnon band gap in a layered perovskite antiferromagnet in coupling with a superconducting resonator. The use of high-quality-factor superconducting resonator allows for coherent interaction with the magnon excitations and the study of unique magnon band gap in a magnetic material with narrow-band microwave measurements. The magnon-photon coupling strength can be tuned from a few tens of megahertz to zero by modifying the magnon band gap location with temperature. At the zero coupling strength state where the resonator mode falls into the magnon band gap, probing the change of photon mode linewidth also allows one to extract the value of magnon band gap using an analytical model. Our results provide a new idea to modify magnon-photon interaction as well as a new approach to study the quantum properties of novel layered magnetic materials from cavity magnonics. To improve the slow temperature tunability of magnon band gap, we anticipate other approaches such as strain or electric field [60–62] for controlling the magnetic properties with high speed and extending the application in coherent information processing.

Acknowledgement. D.S. and M.B. acknowledge the primary financial support through the Center for Hybrid Organic Inorganic Semiconductors for Energy (CHOISE), an Energy Frontier Research Center funded by the Office of Basic Energy Sciences, Office of Science within the U.S. Department of Energy (Hybrid perovskite synthesis, crystal preparation, structural characterization, and motivation of this work). This work was authored in part by the National Renewable Energy Laboratory (NREL), operated by Alliance for Sustainable Energy LLC, for the U.S. Department of Energy (DOE) under contract no. DE-AC36-08GO28308. The views expressed in this article do not necessarily represent the views of the DOE or the U.S. Government. Works at Argonne National Laboratory and University of Illinois and Urbana-Champaign, including the superconducting resonator fabrication, design, ICP chemical analysis, and hybrid magnonics characterization, were supported by the U.S. DOE, Office of Science, Basic Energy Sciences, Materials Sciences and Engineering Division under contract No. DE-SC0022060. Work at UNC-CH were supported by NSF-ECCS 2246254 for the experimental design, data analysis, theoretical analysis, and manuscript preparation. D.S. acknowledges the partial financial support from the Department of Energy grant DE-SC0020992 and the National Science Foundation grant DMR-2143642 for magnetic properties characterization. X.Z. acknowledges support by the National Science Foundation CAREER Award (Grant CBET-2145417) and LEAPS Award (Grant DMR-2137883) for the Raman characterization. Use of the Center for Nanoscale Materials (CNM), an Office of Science user facility, was supported by the U.S. Department of Energy, Office of Science, Office of Basic Energy Sciences,

under Contract No. DE-AC02-06CH11357.

* yili@anl.gov
 † dsun4@ncsu.edu
 ‡ zhwei@unc.edu
 § novosad@anl.gov

- [1] Gershon Kurizki, Patrice Bertet, Yuimaru Kubo, Klaus Mølmer, David Petrosyan, Peter Rabl, and Jörg Schmiedmayer, “Quantum technologies with hybrid systems,” *Proc. Natl. Acad. Sci.* **112**, 3866–3873 (2015).
- [2] A. A. Clerk, K. W. Lehnert, P. Bertet, J. R. Petta, and Y. Nakamura, “Hybrid quantum systems with circuit quantum electrodynamics,” *Nature Phys.* **16**, 257 (2020).
- [3] Dany Lachance-Quirion, Yutaka Tabuchi, Arnaud Glorpe, Koji Usami, and Yasunobu Nakamura, “Hybrid quantum systems based on magnonics,” *Appl. Phys. Express* **12**, 070101 (2019).
- [4] Y. Li, W. Zhang, V. Tyberkevych, W.-K. Kwok, A. Hoffmann, and V. Novosad, “Hybrid magnonics: physics, circuits and applications for coherent information processing,” *J. Appl. Phys.* **128**, 130902 (2020).
- [5] Yi Li, Chenbo Zhao, Wei Zhang, Axel Hoffmann, and Valentyn Novosad, “Advances in coherent coupling between magnons and acoustic phonons,” *APL Mater.* **9**, 060902 (2021).
- [6] Hans Huebl, Christoph W. Zollitsch, Johannes Lotze, Fredrik Hocke, Moritz Greifenstein, Achim Marx, Rudolf Gross, and Sebastian T. B. Goennenwein, “High cooperativity in coupled microwave resonator ferrimagnetic insulator hybrids,” *Phys. Rev. Lett.* **111**, 127003 (2013).
- [7] Maxim Goryachev, Warrick G. Farr, Daniel L. Creedon, Yaohui Fan, Mikhail Kostylev, and Michael E. Tobar, “High-cooperativity cavity qed with magnons at microwave frequencies,” *Phys. Rev. Appl.* **2**, 054002 (2014).
- [8] Yutaka Tabuchi, Seiichiro Ishino, Toyofumi Ishikawa, Rekishu Yamazaki, Koji Usami, and Yasunobu Nakamura, “Hybridizing ferromagnetic magnons and microwave photons in the quantum limit,” *Phys. Rev. Lett.* **113**, 083603 (2014).
- [9] Xufeng Zhang, Chang-Ling Zou, Liang Jiang, and Hong X. Tang, “Strongly coupled magnons and cavity microwave photons,” *Phys. Rev. Lett.* **113**, 156401 (2014).
- [10] Lihui Bai, M. Harder, Y. P. Chen, X. Fan, J. Q. Xiao, and C.-M. Hu, “Spin pumping in electro-dynamically coupled magnon-photon systems,” *Phys. Rev. Lett.* **114**, 227201 (2015).
- [11] Yi Li, Tomas Polakovic, Yong-Lei Wang, Jing Xu, Sergi Lendinez, Zhizhi Zhang, Junjia Ding, Trupti Khaire, Hilal Saglam, Ralu Divan, John Pearson, Wai-Kwong Kwok, Zhili Xiao, Valentine Novosad, Axel Hoffmann, and Wei Zhang, “Strong coupling between magnons and microwave photons in on-chip ferromagnet-superconductor thin-film devices,” *Phys. Rev. Lett.* **123**, 107701 (2019).
- [12] Justin T. Hou and Luqiao Liu, “Strong coupling between microwave photons and nanomagnet magnons,” *Phys. Rev. Lett.* **123**, 107702 (2019).
- [13] Takashi Kikkawa, Ka Shen, Benedetta Flebus, Rembert A. Duine, Ken-ichi Uchida, Zhiyong Qiu, Gerrit E. W. Bauer, and Eiji Saitoh, “Magnon polarons in the spin seebeck effect,” *Phys. Rev. Lett.* **117**, 207203 (2016).
- [14] Cassidy Berk, Mike Jaris, Weigang Yang, Scott Dhuey, Stefano Cabrini, and Holger Schmidt, “Strongly coupled magnon-phonon dynamics in a single nanomagnet,” *Nature Commun.* **10**, 2652 (2019).
- [15] K. An, A. N. Litvinenko, R. Kohno, A. A. Fuad, V. V. Naletov, L. Vila, U. Ebels, G. de Loubens, H. Hurd-equent, N. Beaulieu, J. Ben Youssef, N. Vukadinovic, G. E. W. Bauer, A. N. Slavin, V. S. Tiberkevich, and O. Klein, “Coherent long-range transfer of angular momentum between magnon kittel modes by phonons,” *Phys. Rev. B* **101**, 060407 (2020).
- [16] Jing Xu, Changchun Zhong, Xianjing Zhou, Xu Han, Dafei Jin, Stephen K. Gray, Liang Jiang, and Xufeng Zhang, “Coherent pulse echo in hybrid magnonics with multimode phonons,” *Phys. Rev. Appl.* **16**, 024009 (2021).
- [17] Stefan Klingler, Vivek Amin, Stephan Geprägs, Kathrin Ganzhorn, Hannes Maier-Flaig, Matthias Althammer, Hans Huebl, Rudolf Gross, Robert D. McMichael, Mark D. Stiles, Sebastian T. B. Goennenwein, and Mathias Weiler, “Spin-torque excitation of perpendicular standing spin waves in coupled YIG/Co heterostructures,” *Phys. Rev. Lett.* **120**, 127201 (2018).
- [18] Jilei Chen, Chuanpu Liu, Tao Liu, Yang Xiao, Ke Xia, Gerrit E. W. Bauer, Mingzhong Wu, and Haiming Yu, “Strong interlayer magnon-magnon coupling in magnetic metal-insulator hybrid nanostructures,” *Phys. Rev. Lett.* **120**, 217202 (2018).
- [19] David MacNeill, Justin T. Hou, Dahlia R. Klein, Pengxiang Zhang, Pablo Jarillo-Herrero, and Luqiao Liu, “Gigahertz frequency antiferromagnetic resonance and strong magnon-magnon coupling in the layered crystal crcl₃,” *Phys. Rev. Lett.* **123**, 047204 (2019).
- [20] Yi Li, Wei Cao, Vivek P. Amin, Zhizhi Zhang, Jonathan Gibbons, Joseph Sklenar, John Pearson, Paul M. Haney, Mark D. Stiles, William E. Bailey, Valentine Novosad, Axel Hoffmann, and Wei Zhang, “Coherent spin pumping in a strongly coupled magnon-magnon hybrid system,” *Phys. Rev. Lett.* **124**, 117202 (2020).
- [21] Yoichi Shiota, Tomohiro Taniguchi, Mio Ishibashi, Takahiro Moriyama, and Teruo Ono, “Tunable magnon-magnon coupling mediated by dynamic dipolar interaction in synthetic antiferromagnets,” *Phys. Rev. Lett.* **125**, 017203 (2020).
- [22] A. Sud, C. W. Zollitsch, A. Kamimaki, T. Dion, S. Khan, S. Iihama, S. Mizukami, and H. Kurebayashi, “Tunable magnon-magnon coupling in synthetic antiferromagnets,” *Phys. Rev. B* **102**, 100403 (2020).
- [23] Joseph Sklenar and Wei Zhang, “Self-hybridization and tunable magnon-magnon coupling in van der waals synthetic magnets,” *Phys. Rev. Appl.* **15**, 044008 (2021).
- [24] Mei Li, Jie Lu, and Wei He, “Symmetry breaking induced magnon-magnon coupling in synthetic antiferromagnets,” *Phys. Rev. B* **103**, 064429 (2021).
- [25] M. Harder and C.-M. Hu, “Cavity spintronics: An early review of recent progress in the study of magnon-photon level repulsion,” *Solid State Phys.* **70**, 47 (2018).
- [26] D. D. Awschalom, C.H.R. Du, R. He, J. Heremans, A. Hoffmann, J. Hou, H. Kurebayashi, Y. Li, L. Liu, V. Novosad, J. Sklenar, S. Sullivan, D. Sun, H. Tang, V. Tyberkevych, C. Trevillian, A. W. Tsien, L. Weiss,

- W. Zhang, X. Zhang, L. Zhao, and Ch. W. Zollitsch, “Quantum engineering with hybrid magnonics systems and materials,” *IEEE Trans. Quantum Eng.* **2**, 5500836 (2021).
- [27] Masaya Fukami, Denis R. Candido, David D. Awschalom, and Michael E. Flatté, “Opportunities for long-range magnon-mediated entanglement of spin qubits via on- and off-resonant coupling,” *PRX Quantum* **2**, 040314 (2021).
- [28] H. Y. Yuan, Y. Cao, A. Kamra, R. A. Duine, and P. Yan, “Quantum magnonics: When magnon spintronics meets quantum information science,” *Phys. Rep.* **965**, 1–74 (2022).
- [29] M. Harder, Y. Yang, B. M. Yao, C. H. Yu, J. W. Rao, Y. S. Gui, R. L. Stamps, and C.-M. Hu, “Level attraction due to dissipative magnon-photon coupling,” *Phys. Rev. Lett.* **121**, 137203 (2018).
- [30] Biswanath Bhoi, Bosung Kim, Seung-Hun Jang, Junhoe Kim, Jaehak Yang, Young-Jun Cho, and Sang-Koog Kim, “Abnormal anticrossing effect in photon-magnon coupling,” *Phys. Rev. B* **99**, 134426 (2019).
- [31] Yi-Pu Wang, J. W. Rao, Y. Yang, Peng-Chao Xu, Y. S. Gui, B. M. Yao, J. Q. You, and C.-M. Hu, “Nonreciprocity and unidirectional invisibility in cavity magnonics,” *Phys. Rev. Lett.* **123**, 127202 (2019).
- [32] Isabella Boverter, Christine Dörfinger, Tim Wolz, Rair Macêdo, Romain Lebrun, Mathias Kläui, and Martin Weides, “Control of the coupling strength and linewidth of a cavity magnon-polariton,” *Phys. Rev. Research* **2**, 013154 (2020).
- [33] Jing Xu, Changchun Zhong, Xu Han, Dafei Jin, Liang Jiang, and Xufeng Zhang, “Coherent gate operations in hybrid magnonics,” *Phys. Rev. Lett.* **126**, 207202 (2021).
- [34] N. J. Lambert, J. A. Haigh, S. Langenfeld, A. C. Doherty, and A. J. Ferguson, “Cavity-mediated coherent coupling of magnetic moments,” *Phys. Rev. A* **93**, 021803 (2016).
- [35] Yi Li, Volodymyr G. Yefremenko, Marharyta Lisovenko, Cody Trevillian, Tomas Polakovic, Thomas W. Cecil, Peter S. Barry, John Pearson, Ralu Divan, Vasylyl Tyberkevych, Clarence L. Chang, Ulrich Welp, Wai-Kwong Kwok, and Valentine Novosad, “Coherent coupling of two remote magnonic resonators mediated by superconducting circuits,” *Phys. Rev. Lett.* **128**, 047701 (2022).
- [36] Yutaka Tabuchi, Seiichiro Ishino, Atsushi Noguchi, Toyofumi Ishikawa, Rekishu Yamazaki, Koji Usami, and Yasunobu Nakamura, “Coherent coupling between a ferromagnetic magnon and a superconducting qubit,” *Science* **349**, 405–408 (2015).
- [37] Q. H. Wang and *et al.*, “The magnetic genome of two-dimensional van der waals materials,” *ACS Nano* **16**, 6960 (2022).
- [38] C. Tang, L. Alahmed, M. Mahdi, M. Xiong, J. Inman, N. J. McLaughlin, Ch. Zollitsch, T. H. Kim, C. R. Du, H. Kurebayashi, E. J. G. Santos, W. Zhang, P. Li, and W. Jin, “Ferromagnetic resonance in two-dimensional van der waals magnets: A probe for spin dynamics,” *arXiv* 2301.09822.
- [39] B. Sagarov and D. B. Mitzi, “Organic–inorganic perovskites: Structural versatility for functional materials design,” *Chem. Rev.* **116**, 4558 (2016).
- [40] A. A. Nugroho, Z. Hu, C. Y. Kuo, M. W. Haverkort, T. W. Pi, D. Onggo, M. Valldor, and L. H. Tjeng, “Cross-type orbital ordering in the layered hybrid organic-inorganic compound $(\text{C}_6\text{H}_5\text{CH}_2\text{CH}_2\text{NH}_3)_2\text{CuCl}_4$,” *Phys. Rev. B* **94**, 184404 (2016).
- [41] Ki-Yeon Kim, Garam Park, Jaehun Cho, Joonwoo Kim, June-Seo Kim, Jinyong Jung, Kwonjin Park, Chun-Yeol You, and In-Hwan Oh, “Intrinsic magnetic order of chemically exfoliated 2d ruddlesden–popper organic–inorganic halide perovskite ultrathin films,” *Small* **16**, 2005445 (2020).
- [42] R. D. Willett, C. J. Gómez-García, and B. Twamley, “Long-range order in layered perovskite salts – structure and magnetic properties of $[(\text{ch}_3)_2\text{chch}_2\text{nh}_3]_2\text{CuX}_4$ ($x = \text{Cl}, \text{Br}$),” *Eur. J. Inorg. Chem.* **2012**, 3342 (2012).
- [43] L. J. De Jongh, W. D. Van Amstel, and A. R. Miedema, “Magnetic measurements on $(\text{C}_2\text{H}_5\text{NH}_3)_2\text{CuCl}_4$ - ferromagnetic layers coupled by a very weak antiferromagnetic interaction,” *Physica* **58**, 277 (1972).
- [44] F. Keffer and C. Kittel, “Theory of antiferromagnetic resonance,” *Phys. Rev.* **85**, 329–337 (1952).
- [45] Tôru Moriya, “Anisotropic superexchange interaction and weak ferromagnetism,” *Phys. Rev.* **120**, 91–98 (1960).
- [46] P. Bloembergen, P. J. Berkhout, and J. J. M. Franse, “Static magnetic torque measurements on a system of ferromagnetic layers, coupled by feeble antiferromagnetic interactions; weak ferromagnetic behaviour,” *AIP Conf. Proc.* **10**, 1598 (1973).
- [47] A. N. Bogdanov, A. V. Zhuravlev, and U. K. Röfler, “Spin-flop transition in uniaxial antiferromagnets: Magnetic phases, reorientation effects, and multidomain states,” *Phys. Rev. B* **75**, 094425 (2007).
- [48] Andrew H. Comstock, Chung-Tao Chou, Zhiyu Wang, Tonghui Wang, Ruyi Song, Joseph Sklenar, Aram Amassian, Wei Zhang, Haipeng Lu, Luqiao Liu, Matthew C. Beard, and Dali Sun, “Hybrid magnonics in hybrid perovskite antiferromagnets,” *Nature Commun.* **14**, 1834 (2023).
- [49] Geoffrey M. Diederich, John Cenker, Yafei Ren, Jordan Fonseca, Daniel G. Chica, Youn Jue Bae, Xiaoyang Zhu, Xavier Roy, Ting Cao, Di Xiao, and Xiaodong Xu, “Tunable interaction between excitons and hybridized magnons in a layered semiconductor,” *Nature Nano.* **18**, 23 (2023).
- [50] Takuma Makihara, Kenji Hayashida, G. Timothy Noe II, Xinwei Li, Nicolas Marquez Peraca, Xiaoxuan Ma, Zuanming Jin, Wei Ren, Guohong Ma, Ikufumi Katayama, Jun Takeda, Hiroyuki Nojiri, Dmitry Turchinovich, Shixun Cao, Motoaki Bamba, and Junichiro Kono, “Ultrastrong magnon–magnon coupling dominated by antiresonant interactions,” *Nature Commun.* **12**, 3115 (2021).
- [51] C. W. Zollitsch, S. Khan, V. T. T. Nam, I. A. Verzhbitskiy, D. Sagkovits, J. O’Sullivan, O. W. Kennedy, M. Strungaru, E. J. G. Santos, J. J. L. Morton, G. Eda, and H. Kurebayashi, “Probing spin dynamics of ultrathin van der waals magnets via photon-magnon coupling,” *arXiv* (2022), 2206.02460.
- [52] Elham Easy, Yuan Gao, Yingtao Wang, Dingkai Yan, Seyed M. Gousheghir, Eui-Hyeok Yang, Baoxing Xu, and Xian Zhang, “Experimental and computational investigation of layer-dependent thermal conductivities and interfacial thermal conductance of one- to three-layer wSe_2 ,” *ACS Appl. Mater. Interfaces* **13**, 13063 (2021).
- [53] Antonio Caretta, Rany Miranti, Remco W. A. Havenith, Elia Rampi, Michiel C. Donker, Graeme R. Blake, Matteo Montagnese, Alexey O. Polyakov, Ria Broer, Thomas

- T. M. Palstra, and Paul H. M. van Loosdrecht, “Low-frequency raman study of the ferroelectric phase transition in a layered CuCl_4 -based organic-inorganic hybrid,” *Phys. Rev. B* **89**, 024301 (2014).
- [54] See the Supplemental Information for details.
- [55] L. McKenzie-Sell, J. Xie, C.-M. Lee, J. W. A. Robinson, C. Ciccirelli, and J. A. Haigh, “Low-impedance superconducting microwave resonators for strong coupling to small magnetic mode volumes,” *Phys. Rev. B* **99**, 140414 (2019).
- [56] Y. Xiong, Y. Li, M. Hammami, R. Bidthanapally, J. Sklenar, X. Zhang, H. Qu, G. Srinivasan, J. Pearson, A. Hoffmann, V. Novosad, and W. Zhang, “Probing magnon–magnon coupling in exchange coupled $\text{y}_3\text{fe}_5\text{o}_{12}$ /permalloy bilayers with magneto-optical effects,” *Sci. Rep.* **10**, 12548 (2020).
- [57] Yuzan Xiong, Jerad Inman, Zhengyi Li, Kaile Xie, Rao Bidthanapally, Joseph Sklenar, Peng Li, Steven Louis, Vasyl Tyberkevych, Hongwei Qu, Zhili Xiao, Wai K. Kwok, Valentine Novosad, Yi Li, Fusheng Ma, and Wei Zhang, “Tunable magnetically induced transparency spectra in magnon-magnon coupled $\text{y}_3\text{fe}_5\text{o}_{12}$ /permalloy bilayers,” *Phys. Rev. Appl.* **17**, 044010 (2022).
- [58] Jerad Inman, Yuzan Xiong, Rao Bidthanapally, Steven Louis, Vasyl Tyberkevych, Hongwei Qu, Joseph Sklenar, Valentine Novosad, Yi Li, Xufeng Zhang, and Wei Zhang, “Hybrid magnonics for short-wavelength spin waves facilitated by a magnetic heterostructure,” *Phys. Rev. Appl.* **17**, 044034 (2022).
- [59] S. Khan, O. Lee, T. Dion, C. W. Zollitsch, S. Seki, Y. Tokura, J. D. Breeze, and H. Kurebayashi, “Coupling microwave photons to topological spin textures in Cu_2OSeO_3 ,” *Phys. Rev. B* **104**, L100402 (2021).
- [60] X. Wang, Q. Yang, L. Wang, Z. Zhou, T. Min, M. Liu, and N. X. Sun, “E-field control of the rkky interaction in $\text{fecob/ru/fecob/pmn-pt}$ (011) multiferroic heterostructures,” *Adv. Mater.* **30**, 1803612 (2018).
- [61] H. Yan, Z. Feng, P. Qin, X. Zhou, H. Guo, X. Wang, H. Chen, X. Zhang, H. Wu, C. Jiang, and Z. Liu, “Electric-field-controlled antiferromagnetic spintronic devices,” *Adv. Mater.* **32**, 1905603 (2020).
- [62] C. Liu, Y. Luo, D. Hong, S. S.-L. Zhang, H. Saglam, Lin Y. Li, Y. and, B. Fisher, J. E. Pearson, J. S. Jiang, H. Zhou, J. Wen, A. Hoffmann, and A. Bhattacharya, “Electric field control of magnon spin currents in an antiferromagnetic insulator,” *Sci. Adv.* **7**, eabg1669 (2021).